Symmetric Electret-Based Vibration Energy Harvesters with Curved-Beam Hinges

Dooyoung Hah
Department of Electrical and Electronics Engineering
Abdullah Gül University
Kayseri, Türkiye
dooyoung.hah@agu.edu.tr

2023 Symposium on Design, Test, Integration & Packaging of MEMS/MOEMS (DTIP) | 979-8-3503-4131-7/23/$31.00 ©2023 IEEE | DOI: 10.1109/DTIP58682.2023.10267953

***Abstract*—Broadband power spectral characteristics are desirable in vibration energy harvesters, and it can be achieved by employing curved-beam hinges, which exhibit force-displacement nonlinearity. Via numerical analysis by using stochastic differential equations and colored-noise inputs, this study shows that a symmetric configuration of the curved-beam hinges in electret-based harvesters can produce higher (up to 8% more) power outputs than an asymmetric one. It also presents that the harvesters with curved-beam hinges can produce higher (up to 4.4 times) power outputs than those with straight hinges when the vibration magnitude is 0.05*g*.**

Keywords—energy harvester, mechanical vibration, nonlinear spring, curved beam, electret

I. Introduction

Mechanical vibrations are ubiquitous while most of them are wasted. Vibration energy harvesters (VEHs) are the devices that convert these vibrations into electricity. One of the important aspects to be considered in the VEH design is its frequency response characteristics. It is desirable to match them to those of the typical vibration sources, i.e. broadband and stochastic, which can be described as colored noise. Various methods have been attempted so far to broaden the spectra of VEHs, such as Duffing oscillators [1], arrays of single degree-of-freedom (DOF) structures [2], multi-DOF structures [3], and nonlinear springs [4]. Among these methods, nonlinear springs are advantageous, especially for the applications that have limited footprints. Spring nonlinearity can be reinforced by adding an initial curve to a clamped-clamped beam, which makes it a Duffing-Holmes oscillator, featuring second- and third-order nonlinearities [5].

Recently, we also have reported on the pre-shaped curved-beam hinges, more specifically on their colored-noise responses [6-7]. In these reports, via analytical study by using stochastic differential equations, we have shown that electret-based VEHs (eVEHs) with curved-beam hinges can harvest higher electric power than the ones with straight-beam hinges for a certain range of vibration magnitudes. It was also learned that it is the other way around at high vibration magnitudes (e.g. at 0.1*g*; *g*: gravitational acceleration), i.e. the eVEHs with straight-beam hinges are more efficient. The motivation of the current work starts from this point; it is to search for a device configuration that produces higher power output at high vibration magnitudes.

The structure of the eVEHs in the previous studies was based on a balanced-comb-drive configuration [8]. When a proof mass moves in response to external vibration, engagements of comb-drive fingers change, inducing redistribution of charges in the electrets, which are formed as a dielectric layer on the sides of the comb fingers. This charge redistribution results in the electric power generation. Although the device configuration was symmetric in almost every aspect in those works, including the comb-drives and the loads, curved-beam hinges were incorporated asymmetrically; i.e. initial curves were towards the same direction for all of the springs as illustrated in Fig. 1 (bottom). In this study, a slight modification is rendered in the configuration, i.e. the symmetry is completed by reversing the initial curves towards the opposite direction for a half of the hinges as depicted in Fig. 1 (top). It will be shown that such a symmetric configuration cancels the second-order nonlinearity, making the device a Duffing oscillator, which showed better efficiency at high vibration magnitudes.

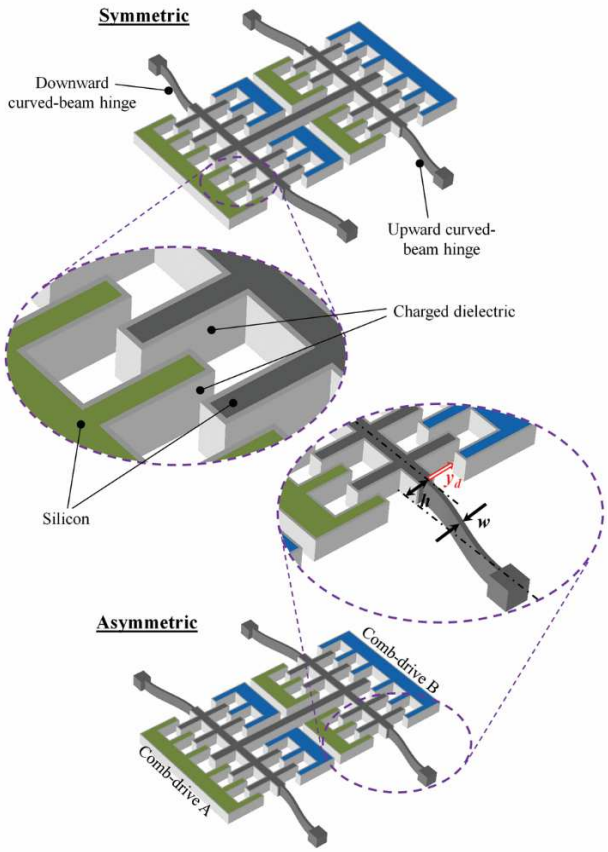

Fig. 1. Sketches of eVEHs. (Top) symmetric and (bottom) asymmetric curved-hinge configurations. A proof mass is omitted in the sketch.

II. Symmetric Curved-Beam Hinge Configuration

The relationship between the restoring force (F_r) and the beam-center displacement (y_d, see Fig. 1) of a curved-beam

hinge, for the asymmetric-hinge eVEHs as well as for the upward-curve hinges in the symmetric-hinge devices, can be expressed as,

$$F_{r,asym}(y_d) = k_1 y_d + k_2 y_d^2 + k_3 y_d^3 = F_{r,up}(y_d) \quad (1)$$

where k_1, k_2 and k_3 are a linear, a quadratic, and a cubic spring constant, respectively. The spring constants are dependent on the beam width (w) and the beam height (h, see Fig. 1) as follows [7].

$$k_1 = \frac{\pi^4 EwT}{12l^3}(2w^2 + 3h^2) \quad (2a)$$

$$k_2 = \frac{3\pi^4 EwTh}{8l^3} \quad (2b)$$

$$k_3 = \frac{\pi^4 EwT}{8l^3} \quad (2c)$$

where E, T and l are Young's modulus of the beam (179 GPa for silicon), a beam thickness, and a beam length, respectively. The F_r vs. y_d relationship for the downward-curve hinges becomes,

$$F_{r,dn}(y_d) = k_1 y_d - k_2 y_d^2 + k_3 y_d^3, \quad (3)$$

which makes the overall F_r vs. y_d relationship in the symmetric-hinge device as follows.

$$F_{r,sym,total}(y_d) = \frac{N_s}{2}\left[F_{r,up} + F_{r,dn}\right] = N_s\left(k_1 y_d + k_3 y_d^3\right) \quad (4)$$

where N_s is the number of springs. Equation (4) shows that the characteristics of the symmetric-hinge VEHs become similar to those of the straight-hinge devices, except the fact that the linear spring constant (k_1) can be adjusted by the beam heights.

Fig. 2 compares the F_r vs. y_d relationships between the symmetric and the asymmetric devices for various beam heights, which are expressed in terms of the critical beam height (h_{cr}). h_{cr} is the beam height, from which a single curved-beam hinge starts to show bistability, and is found as [9]

$$h_{cr} = \frac{4}{\sqrt{3}} w \quad (5)$$

For the w value of 20 μm, h_{cr} is equal to 46.2 μm. The characteristics of the asymmetric devices (Fig. 2b) show that a high value of h results in low $|F_r|$ when y_d is negative (it generates high F_r for $y_d > 0$). A snapping behavior (for $h > 0.5h_{cr}$) and bistability (for $h > h_{cr}$) can be also observed in the case of asymmetric devices. On the other hand, the characteristics of the symmetric devices (Fig. 2a) show a symmetry about $y_d = 0$ without snapping or bistability. From these, it can be understood that the asymmetric hinge configuration favors one direction of the proof-mass movement over the other direction while the symmetric one will show a symmetric movement behavior. In certain conditions, asymmetric movements with a clear advantage in one direction can produce wider range of motion. In other circumstances, symmetric movements can be more beneficial. This inference will be examined with the results in the following sections.

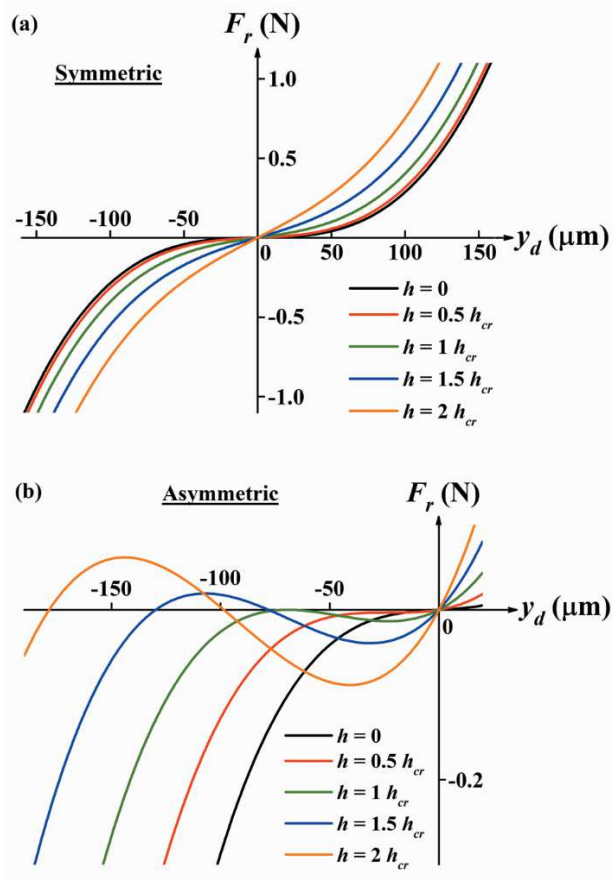

Fig. 2. Restoring force (F_r) vs. beam-center displacement (y_d) of (a) symmetric and (b) asymmetric curved-hinges for various curved-beam heights (h). h are expressed in terms of the critical beam height (h_{cr}).

III. Device Model and Analysis Method

Analysis of the eVEHs was carried out based on the following stochastic differential equations [6-7].

$$dy_d = y_v dt \quad (6)$$

$$dy_v = y_a dt = -\frac{1}{m}\left[c_d y_v + F_r - \frac{1}{2y_v}\frac{dU_e}{dt} - \sigma\frac{dW_t}{dt}\right]dt \quad (7)$$

$$dV = \frac{1}{C}\left[(V_S - V)dC - \frac{V}{R_L}dt\right] \quad (8)$$

where y_v is the beam-center velocity, t the time, y_a the beam-center acceleration, m a proof mass (2.5 g), c_d a damping coefficient (1 g/s), U_e the electrostatic potential energy, σ the diffusion coefficient that is proportional to the external vibration magnitude (a_{ext}), W_t the Wiener process that models the stochastic vibration input, C the capacitance of a comb (comb-drive A or B, Fig. 1), V the voltage on a comb, V_S the surface potential (200 V), i.e. the charging voltage of the electrets, and R_L the load resistance. W_t was generated by processing a random uncorrelated time series through a low pass filter (cutoff: 500 Hz), becoming a colored noise. To obtain more accurate results, five hundred different time series, each with the length of forty million, were applied to a device as an input. Equations (1)-(8) were used to produce all the pertinent series, and the average power was calculated from the voltage time series. Silicon (thickness: 400 μm) was considered as the material of the structure. The number of springs (N_S) was eight for a single device.

IV. Results and Discussion

Fig. 3 compares the phase portraits between the symmetric and the asymmetric devices when a_{ext} (rms) is 0.15g. In the case of the asymmetric device, movement is favored towards the negative y_d as expected, and bistability can be observed. On the other hand, the symmetric device exhibits a symmetric behavior, also as expected. With the given condition, the symmetric device exhibits higher displacements and velocities than the asymmetric one.

Fig. 4 presents the calculated average electric power as a function of the beam heights for both types of the devices and at different vibration magnitudes (a_{ext}). Analysis was carried out with various load conditions, and only the results producing the highest power output at the specific a_{ext} value are included in the figure. It can be observed that in the case of the symmetric devices, curved-beam hinges result in higher power outputs than the straight hinges (i.e. h = 0) for the range of a_{ext} values considered in the study (0.05g–0.2g). The beam height value resulting in the highest power decreases as a_{ext} increases. It can be also observed that the advantage of the curved beams becomes weaker as a_{ext} increases. On the other hand, in the case of the asymmetric devices, the straight hinges ended up becoming the most efficient one except the case when a_{ext} is 0.05g. Table I summarizes the highest electric power output that can be obtained at each vibration magnitude for both devices. It can be concluded that the devices with the symmetric hinge configuration can produce higher power (as much as 8% more) than the asymmetric configuration for the vibration magnitude range of 0.1g–0.2g. When compared to the straight-hinge device, the symmetric device can produce as much as 4.4 times higher power (@ 0.05g).

Examples of the power spectral density (PSD) graphs are presented in Fig. 5 for both types of the devices at optimum load conditions. As expected, the spectra show substantial nonlinearity and broadband characteristics. In the case of the symmetric devices, spectra tend to shift towards the higher frequency and the peaks become narrower as the beam height increases. For asymmetric devices, however, spectra tend to shift towards the lower frequency as h increases. It can be also observed that, at 0.15g, the power increases as h increases from 0 to 1h_{cr} in the symmetric device, which is the opposite in case of the asymmetric device.

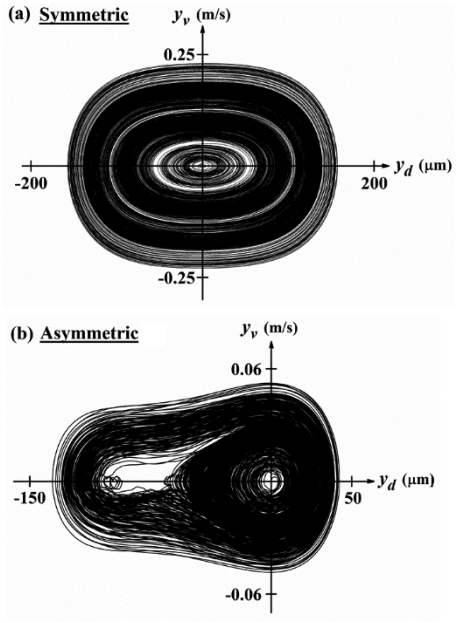

Fig. 3. Phase portraits (velocity vs. displacement) of the eVEHs with (a) symmetric and (b) asymmetric curved-beam hinge configurations. a_{ext} = 0.15g, R_L = 10 MΩ, and h = 1.2 h_{cr}.

TABLE I. Comparison of Maximum Electric Power Outputs

Vibration magnitude (a_{ext} in g)	*Symmetric configuration*		*Asymmetric configuration*	
	Power (mW)	*h (×h_{cr})*	*Power (mW)*	*h (×h_{cr})*
0.05	0.0921	1.1	0.0994	1.0
0.10	0.310	0.9	0.289	0.0
0.15	0.383	0.7	0.358	0.0
0.20	0.470	0.7	0.435	0.0

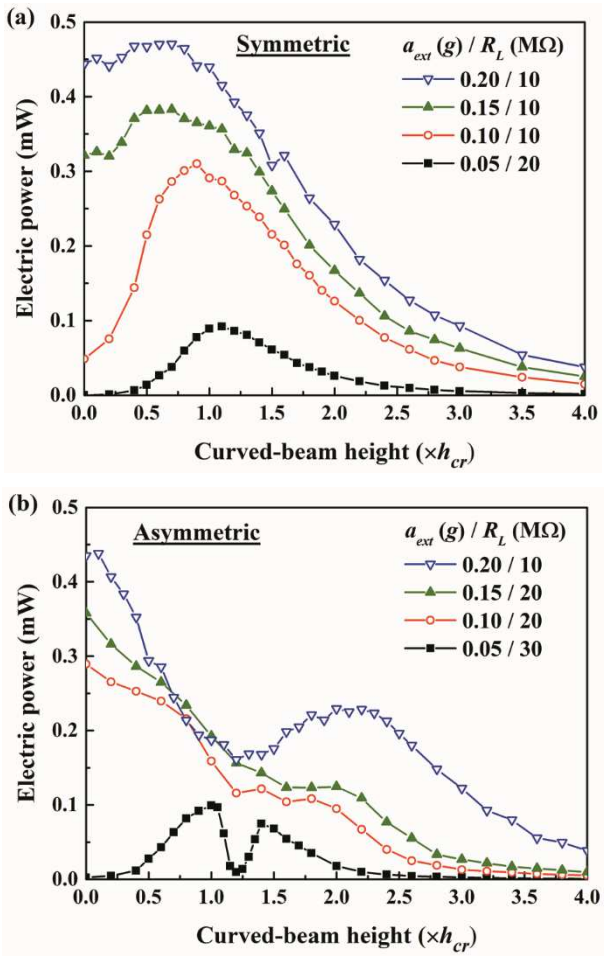

Fig. 4. Calculated average electric power of eVEHs at various vibration magnitudes (a_{ext}). (a) Symmetric and (b) asymmetric curved-hinge configurations. Cases with the optimum load conditions (R_L) are shown.

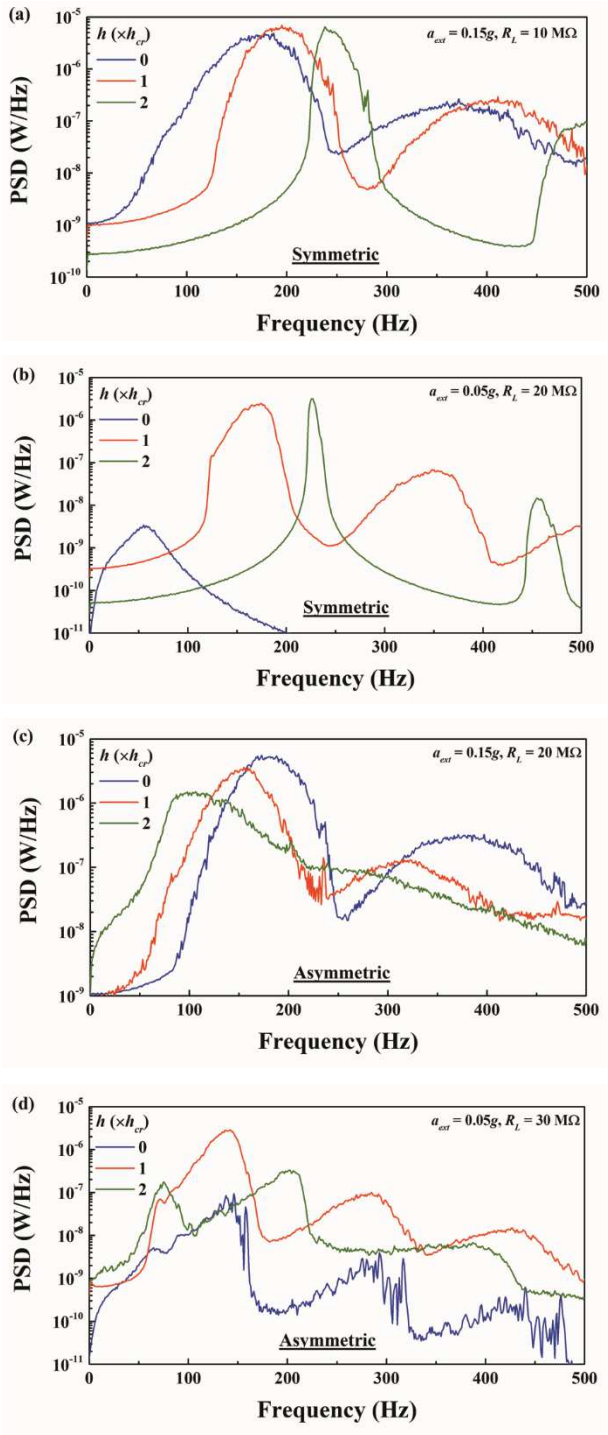

Fig. 5. Electric power spectral density (PSD) for various beam heights (h) and vibration magnitudes (a_{ext}). The values of a_{ext} and the load resistances are given in each graph. (a-b) Symmetric and (c-d) asymmetric curved-beam hinge configurations.

V. Conclusion

Symmetrically configured curved-beam hinges were compared to the asymmetrical ones in electret-based VEHs through numerical simulation. It was learned that at high vibration magnitudes (0.1g–0.2g), symmetrical devices can produce higher power output than the asymmetrical ones.

References

[1] T. L. Pereira, A. S. de Paula, A. T. Fabro AT, and M. A. Savi, "Random effects in a nonlinear vibration-based piezoelectric energy harvesting system," Int. J. Bifurcation and Chaos, vol. 29, p. 1950046, 2019.

[2] Z. Xiao, T. Q. Yang, Y. Dong, and X. C. Wang, "Energy harvester array using piezoelectric circular diaphragm for broadband vibration," Appl. Phys. Lett., vol. 104, p. 223904, 2014.

[3] X. Li, K. Yu, D. Upadrashta, and Y. Yang, "Multi-branch sandwich piezoelectric energy harvester: Mathematical modeling and validation," Smart Mater. and Struct., vol. 28, p. 035010, 2019.

[4] A. Hajati and S. G. Kim, "Ultra-wide bandwidth piezoelectric energy harvesting," Appl. Phys. Lett., vol. 99, p.083105, 2011.

[5] H. Du, F. S. Chau, and G. Zhou, "Harmonically-driven snapping of a micromachined bistable mechanism with ultra-small actuation stroke," J. Microelectromech. Syst., vol. 27, pp.34-39, 2018.

[6] D. Hah, "Effects of curved-beam heights to harvested energy in a blanaced comb-drive configuration," Digests Symp. on Design, Test, Integration & Packaging of MEMS and MOEMS (DTIP), Paris, France, pp. 1-4, 2021.

[7] D. Hah, "Analysis of electret-based vibration energy harvesting devices with curvedbeam hinges," J. Intel. Mater. Syst. Strut., in press.

[8] H. Honma, Y. Tohyama, and H. Toshiyoshi, "A 1.3 milliwatts electrostatic vibrational energy harvester with minimal reactive power through reduced internal straycapacitances," Digests Transducers 2019 – Eurosensors XXXIII, Berlin, Germany, pp.362-365, 2019.

[9] J. Qiu, J. H. Lang, and A. H. Slocum, "A curved-beam bistable mechanism," J. Microelectromech. Syst., vol. 13, pp. 137-146, 2